



저작자표시-변경금지 2.0 대한민국

이용자는 아래의 조건을 따르는 경우에 한하여 자유롭게

- 이 저작물을 복제, 배포, 전송, 전시, 공연 및 방송할 수 있습니다.
- 이 저작물을 영리 목적으로 이용할 수 있습니다.

다음과 같은 조건을 따라야 합니다:



저작자표시. 귀하는 원저작자를 표시하여야 합니다.



변경금지. 귀하는 이 저작물을 개작, 변형 또는 가공할 수 없습니다.

- 귀하는, 이 저작물의 재이용이나 배포의 경우, 이 저작물에 적용된 이용허락조건을 명확하게 나타내어야 합니다.
- 저작권자로부터 별도의 허가를 받으면 이러한 조건들은 적용되지 않습니다.

저작권법에 따른 이용자의 권리는 위의 내용에 의하여 영향을 받지 않습니다.

이것은 [이용허락규약\(Legal Code\)](#)을 이해하기 쉽게 요약한 것입니다.

[Disclaimer](#)

**Removal of filamentous algae by positively  
charged bubble flotation: a comparative study  
with spherical/ spherical-like shapes**

**By**

**Bui Thi Thuy**

**Supervisor: Professor Moo-young Han**

**A dissertation submitted in partial fulfillment of the requirements for  
the degree of Master in Department of Civil and Environmental  
Engineering, Seoul National University.**

**Department of Civil and Environmental Engineering**

**College of Engineering**

**Seoul National University**

## **Abstract**

# **Removal of filamentous algae by positively charged bubble flotation: a comparative study with spherical/ spherical-like shapes**

**Bui Thi Thuy**

Dept. of Civil and Environmental Engineering

College of Engineering

Seoul National University

The objective of this study was to compare removals of filamentous algae with spherical/ spherical-like algae during charged bubble flotation process, optimize operation conditions for better removal of filamentous algae and observe the change of algal morphology to identify mechanisms underlying the efficiency of flotation with positively charged bubbles. Three selected shapes in this research are spherical (*Microcystis sp.*), oval (*Chlamydomonas angulosa*) and filamentous algae (*Phormidium sp.*), cultured in the laboratory under certain cultivated conditions. Physical

properties of three differing algae were understood as morphology, size distribution and zeta potential in various pH. Under pH conditions of 4.5~7, all algae species showed negative charges; -10 mV for filamentous shape, ~ -20 mV for oval shape and ~ -40 mV for spherical shape. The size of these shapes ordered increasingly as spherical < oval < filamentous algae. Removal of differing algal shapes were conducted by the batch dissolved air flotation (BDAF) method with bubble generation from saturated pressure of 6 bars, in the presence of aluminium at 30% of bubble rate. Filamentous algae presented the greatest results (i.e. 86% for cell removal and ~93% for chlorophyll *a* reduction) when comparing to spherical/ spherical-like algae (i.e. ~75% for cell removal and ~80% for chlorophyll *a* reduction). For better filamentous algal removal, the optimum operational condition was also investigated. Bubbles were generated at two levels of saturated pressure (3 bars, 6 bars) and measured at different bubble concentrations (10%, 20%, and 30%), in the absence and presence of coagulants. Bubbles averaging 30  $\mu\text{m}$  and 45  $\mu\text{m}$  in size were observed at zeta potentials of -30 mV~+27 mV. We obtained optimal filamentous algal removal with positively charged bubble flotation at a 30% bubble rate at >16 mV and a bubble size of 30  $\mu\text{m}$ , with removal of up to 85% and 93% of cells and chlorophyll *a*, respectively. Also, by positively charged bubble flotation, only filamentous cell changed its size arrangement and promoted spherically or ovals being to adopt with the stress environment. We also demonstrated the efficacy of using positively charged bubbles to remove filamentous cells and the

importance of positively charged bubbles in the rarely reported interaction between bubbles and chain-like algae.

**Keywords:** Bubble generation conditions, chain-like algae, filamentous algae removal, flotation, positively charged bubble, zeta potential

**Student number: 2012-23968**

## Contents

<b>List of Tables</b> .....	I
<b>List of Figures</b> .....	II
<b>Chapter 1. INTRODUCTION</b> .....	1
<b>1.1. Background</b> .....	1
<b>1.2. Objectives</b> .....	3
<b>1.3. Dissertation structure</b> .....	4
<b>Chapter 2. BUBBLE CHARACTERISTIC AND BATCH TESTING</b> .....	11
<b>2.1. Introduction</b> .....	11
<b>2.2. Bubble characteristics</b> .....	12
<b>2.2.1. Measurement methods</b> .....	12
<b>2.2.2. Bubble’s zeta potential and size distribution</b> .....	14
<b>2.3. Batch testing</b> .....	17
<b>Chapter 3. REMOVAL OF DIFFERING ALGAL SHAPES BY CHARGED BUBBLE FLOTATION</b> .....	21
<b>3.1. Introduction</b> .....	21
<b>3.2. Materials and method</b> .....	22
<b>3.2.1. Algal culturing</b> .....	22
<b>3.2.2. Experimental setup</b> .....	24
<b>3.3. Results and discussion</b> .....	25
<b>3.3.1. Algal properties</b> .....	25
<b>3.3.2. Removal efficiencies</b> .....	27
<b>3.4. Summary</b> .....	30

Chapter 4. OPTIMAL CONDITION FOR BETTER REMOVAL OF FILAMENTOUS ALGAE .....	33
<b>4.1. Introduction</b> .....	33
<b>4.2. Materials and Methods</b> .....	34
<b>4.2.1. Phormidium sp. culture and its properties</b> .....	34
<b>4.2.2. Bubble generation and batch testing</b> .....	34
<b>4.3. Experimental results</b> .....	35
<b>4.3.1. Characteristics of Phormidium sp.</b> .....	35
<b>4.3.2. Removal efficiencies</b> .....	36
<i>4.3.2.1. Effects of the zeta potential of the bubble</i> .....	36
<i>4.4.2. The effects of bubble size</i> .....	40
<i>4.4.3. The effects of bubble concentration</i> .....	42
<b>4.4. Summary</b> .....	44
Chapter 5. THE CHANGE OF ALGAL MORPHOLOGY BY POSITIVELY CHARGED BUBBLE FLOTATION.....	47
<b>5.1. Change of size distribution</b> .....	47
<b>5.2. Change of algal shapes</b> .....	50
<b>5.3. The breakup of filamentous algae and possible mechanism of removal</b> .....	51
<b>5.4. Summary</b> .....	55
Chapter 6. CONCLUSIONS .....	57

# List of Tables

**Table 2.1.** Average bubble size and pressure

**Table 3.1.** Composition of JM (Javorski's Medium)

**Table 3.2.** BDAF tests for removal of differing algal shapes

**Table 4.1.** Summary of experimental conditions for better removal

**Table 4.2.** Morphology of *Phormidium* sp. cultivated in flasks and the concentration used for flotation experiments

**Table 4.3.** Mobility of *Phormidium* sp. before and after positively charged bubble flotation

# List of Figures

**Figure 1.1.** Dissertation structure

**Figure 2.1.** Schematic diagram to measure zeta potential of bubble

**Figure 2.2:** Schematic diagram of online particle counting method

**Figure 2.3:** Zeta potential of bubble in various coagulant dose

**Figure 2.4:** Bubble zeta potential in the presence of metal solutions (by Han and Dockko, 2004).

**Figure 2.5:** Schematic diagram of algae removal by Batch DAF

**Figure 3.1:** The shape of three algal species under cultivated condition

**Figure 3.2:** Initial size distribution of three algal species

**Figure 3.3:** Zeta potential of three algal shapes

**Figure 3.4:** Cell removals of differing algal shapes

**Figure 3.5:** Chlorophyll *a* reduction of differing algal shapes

**Figure 4.1:** Bubble zeta potential in the presence of aluminum ( $Al^{3+}$ ).

**Figure 4.2:** *Phormidium* sp. removal by flotation method

**Figure 4.3:** Zeta potential of *Phormidium* sp. in flotation process

**Figure 4.4:** Cell removal of *Phormidium* sp. with different bubble sizes

**Figure 4.5:** Chlorophyll *a* reduction of *Phormidium* sp. with different bubble sizes.

**Figure 4.6:** Cell removal of *Phormidium* sp. at different bubble rates

**Figure 4.7:** Chlorophyll *a* reduction of *Phormidium* sp. at different bubble rates.

**Figure 5.1:** The change of size distribution of spherical algae by flotation

**Figure 5.2:** The change of size distribution of oval algae by flotation

**Figure 5.3:** The change of size distribution of filamentous algae by flotation

**Figure 5.4:** The change of algae shapes/color

**Figure 5.5:** Microscopic images of broken cells

**Figure 5.6:** Collision of a *Phormidium* sp. filament and a positively charged bubble.

**Figure 5.7:** Net force exerted on the chain-like cells by the positively charged bubble

# Chapter 1. INTRODUCTION

## 1.1. Background

Algal blooms cause harmful effects on human and environment so that they are the major concern in water treatment (Aktas, 2012). They may occur in freshwater as well as marine environments and the toxins produced by blooms can adversely affect human health in waters used for recreation, drinking purposes, ecosystem (Paerl, 2001a). Morphology of algae including shape and size may have impacts on the performance of flotation process when considering the bubble-cell attachment, in addition, algae removals are also dependent on algal species (Jarvis, 2009; Teixeira, 2010). Some common algal shapes are addressed in terms of spherical, oval and filamentous forms. In particular, filamentous algae at the base of the water column in fresh watersheds form a periphyton community under high light conditions, consisting of series of cells joined end-to-end, giving them a thread-like appearance (Edward G. Bellinger and Sigeo, 2010). In lakes or ponds, these normally develop into massive surface populations known as “pond moss” or “pond scum,” especially in summer (Edward G. Bellinger and Sigeo, 2010; Hilda Canter-Lund and WG-Lund, 1996; Paerl, 2001b; Sze, 1998).

Dissolved air flotation (DAF) has proven its effectiveness, become a well-established water treatment and separation processes (Bare and others,

1975; Gao, 2010a; Gao, 2010b; Han, 1998; Hanotu and others, 2012; Jarvis, 2009; Phoochinda, 2003; Wang, 2008) . It is widely employed as a novel technology to treat algae due to its advances of floatable tendency by forming very small flocs (Haarhoff, 2001; Teixeira, 2006). DAF easily separates the low-density particles (algae and small flocs) thus it can be an alternative of sedimentation process (Kwon, 2004). The efficiency of flotation process is dependent upon the collision of bubble and particles which is affected by certain parameters with respect to sizes and zeta potentials of bubble and particle (Han, 2004; Han, 2006; Phoochinda, 2003; Taki, 2008). Positively charged bubbles collide with particles to form small flocs, called bubble-particle attachment (Gao, 2010a; Gao, 2010b; Haarhoff, 2001; Kwon, 2004). Characteristics of algae affecting treatment efficiency are morphology, motility, surface charge, cell density and the extracellular organic matter (EOM) composition, the number of cell or concentration of chlorophyll a (Henderson, 2008a). It's demonstrated that at natural conditions, algae are negatively charged therefore it requires positive bubbles for higher removal efficiency (Han, 2001a; Henderson, 2010). When employing positive bubble generated from a saturation pressure of 6 bars with covalent metal ion as a coagulant, higher removal efficiency was obtained compared to the conventional DAF process (Malley, 1995). It therefore implies that positively charged bubble flotation is the viable tool for algae control in water treatment area.

## 1.2. Objectives

This study focuses on behaviours of chain-like algae by positively charged bubble flotation in comparison with spherical or spherical-like algae. The aim of this study therefore are to:

1) Compare removal efficiencies in terms of the number of the cells and chlorophyll *a* reduction of filamentous algae with spherical or spherical-like algae by charged bubble flotation;

2) Optimize operation conditions of flotation for better chain-like algae removals, in which bubble were generated at the differences of:

- a) Zeta potential values (in the absence and presence of aluminum with concentration of 0, 0.5, 1 and 5 mg/L);
- b) Bubble sizes which are generated from different pressure (i.e. 3 bars and 6 bars);
- c) Bubble rates injected to the reactor (i.e. 10%, 20% and 30% of bubble injection) and;

3) Assess effect of algal shape (spherical, oval and chain-like shape, represented by *Microcystis sp.*, *Chlamydomonas angulosa* and *Phormidium sp.*, respectively) on change of algal morphology (i.e. shape and size distribution) and possible mechanism for filamentous algal removal by positively charged bubble flotation.

The study also focuses on reduction of the number of cells, interaction between algae and bubble to remove chlorophyll *a*, the best existence formation of structure in the stress environment.

### 1.3. Dissertation structure

The contents of this study is arranged in 6 chapters (see in Fig. 1.1).

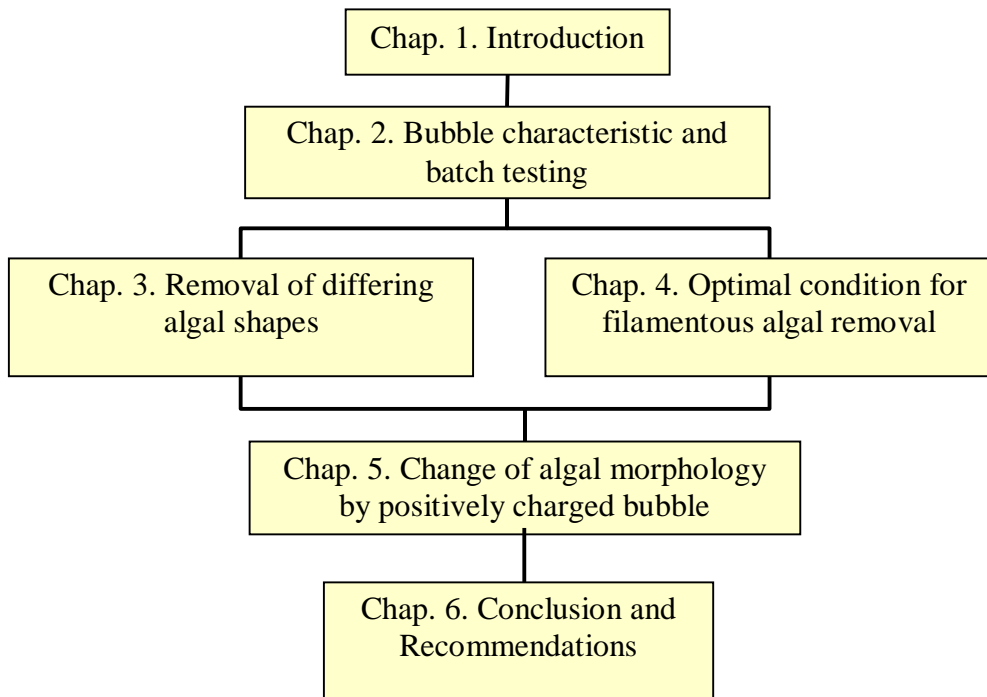


**Figure 1.1.** Dissertation structure

Chapter 1 includes some sections such as the general introduction, objectives and dissertation. Chapter 2 indicates the method of bubble generation with its characteristics measurement and batch testing. Chapter 3 reports removal efficiencies of three differing algal shapes. Chapter 4

investigates the optimal operation conditions for better filamentous algal removal. Chapter 5 observes the change of algal morphology (i.e. size distribution and shape) to show the possible mechanism for removal of filamentous algae by positively charged bubble flotation. And finally, chapter 6 is the conclusion of this study.

## REFERENCES

Aktas, T.S., Takeda, F., Maruo, C., Nisimura, O., A comparison of zeta potential and behaviors of cyanobacteria and algae. *Desalination and Water Treatment*, 2012. 48: p. 294-301.

Paerl, H.W., Fulton, R. S., Moisander, P. H., Dyble, J., Harmful freshwater algal blooms, with an emphasis on cyanobacteria. *ScientificWorldJournal*, 2001. 1: p. 76-113.

Bare, W.F., N.B. Jones, and E.J. Middlebrooks, Algae removal using dissolved air flotation. *J Water Pollut Control Fed*, 1975. 47(1): p. 153-69.

Han, M.Y., Dockko, S., Zeta potential measurement of bubbles in DAF process and its effect on removal efficiency. *KSCE Journal of Civil Engineering*, 1998. 2(No 4): p. 461-466.

Phoochinda, W., White, D. A., Removal of algae using froth flotation. *Environmental Technology*, 2003. 24(1): p. 87-96.

Wang, Y.H., Wang, Q. S., Wu, Y. B., Yue, L., Yang, J. K., Treatment of high algae-laden water by step-recycle counter current flotation. *Huan Jing Ke Xue*, 2008. 29(11): p. 3071-6.

Jarvis, P., Buckingham, P., Holden, B., Jefferson, B., Low energy ballasted flotation. *Water Research*, 2009. 43(14): p. 3427-34.

Gao, S., Du, M., Tian, J., Yang, J., Ma, F., Nan, J., Effects of chloride ions on electro-coagulation-flotation process with aluminum electrodes for algae removal. *Journal of Hazard Mater*, 2010. 182(1-3): p. 827-34.

Gao, S., Yang, J., Tian, J., Ma, F., Tu, G., Du, M., Electro-coagulation-flotation process for algae removal. *Journal of Hazard Mater*, 2010. 177(1-3): p. 336-43.

Hanotu, J., H.C. Bandulasena, and W.B. Zimmerman, Microflotation performance for algal separation. *Biotechnology and Bioengineering*, 2012. 109(7): p. 1663-73.

Haarhoff, J., Edzwald, J. K., Modelling of floc-bubble aggregate rise rates in dissolved air flotation. *Water Science and Technology*, 2001. 43(8): p. 175-84.

Teixeira, M.R., Rosa, M. J., Integration of dissolved gas flotation and nanofiltration for *M. aeruginosa* and associated microcystins removal. *Water Research*, 2006. 40(19): p. 3612-20.

Kwon, S.B., Ahn, H. W., Ahn, C. J., Wang, C. K., A case study of dissolved air flotation for seasonal high turbidity water in Korea. *Water Science and Technology*, 2004. 50(12): p. 245-53.

Han, M.Y., Ahn, H. J., Shin, M. S., Kim, S. R., The effect of divalent metal ions on the zeta potential of bubbles. *Water Science and Technology*, 2004. 50(8): p. 49-56.

Han, M.Y., Kim, M. K., Ahn, H. J., Effects of surface charge, micro-bubble size and particle size on removal efficiency of electro-flotation. *Water Science and Technology*, 2006. 53(7): p. 127-32.

Taki, K., Seki, T., Mononobe, S., Kato, K., Zeta potential measurement on the surface of blue-green algae particles for micro-bubble process. *Water Science and Technology*, 2008. 57(1): p. 19-25.

Henderson, R., Parsons, S. A., Jefferson, B., The impact of algal properties and pre-oxidation on solid-liquid separation of algae. *Water Research*, 2008. 42(8-9): p. 1827-45.

Han, M., Kim, W., Dockko, S., Collision efficiency factor of bubble and particle ( $\alpha_{bp}$ ) in DAF: theory and experimental verification. *Water Science and Technology*, 2001. 43(8): p. 139-144.

Henderson, R.K., Parsons, S. A., Jefferson, B., The impact of differing cell and algogenic organic matter (AOM) characteristics on the coagulation and flotation of algae. *Water Research*, 2010. 44(12): p. 3617-24.

Malley, J.P., The use of selective and direct DAF for removal of particulate contaminant in drinking water treatment. *Water Science and Technology*, 1995. 31: p. 49-57.

Teixeira, M.R., Sousa, V., Rosa, M. J., Investigating dissolved air flotation performance with cyanobacterial cells and filaments. *Water Research*, 2010. 44(11): p. 3337-44.

## Chapter 2. BUBBLE CHARACTERISTIC AND BATCH TESTING

### 2.1. Introduction

Bubble generation is the most important step in flotation process and it decides the effectiveness of flotation performance. The collision between bubble and particle has the strongest impact on the removal efficiencies. In the collision mechanism of bubble and particle, it was reported that the opposite charges and similar size would enhance removal efficiencies (Han, 2006; Han, 2001b). It therefore confirms that the characterizations of bubble affecting the effectiveness of flotation process in which bubble's zeta potential and bubble's size are known as the most important ones. Indeed, many researches about the charges of bubble has been highlighted on removal of contaminant, for example algae, turbidity, sediments in natural water basin (Han M. Y., 2006; Han, 1998). Furthermore, in order to increase removal, the size, the charge and the concentration of bubble have to be effectively controlled. To do that, the bubble characteristics measurement must be determined by accurate methods. This chapter hence describes the methods to measure zeta potential and the size of bubble by image analysis system and online particle counting, respectively.

## 2.2. Bubble characteristics

### 2.2.1. Measurement methods

Micro-bubbles were generated at saturated pressures in the presence of coagulants in 1 L de-ionized water (Kim, 2012). Zeta potential was measured with an electrophoresis cell, video camera, and video image analyzer and provided in Figure 2.1 (Han, 2001b).

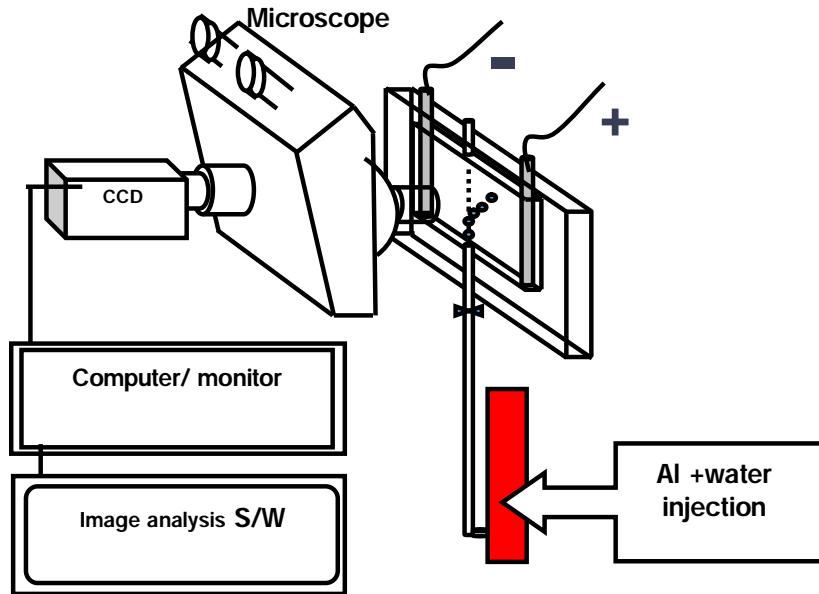


**Figure 2.1:** Schematic diagram to measure zeta potential of bubble

This system measured electrophoretic mobility; zeta potential was calculated by using Smoluchowski's equation (Han, 1998).

$$\zeta = \frac{\mu K A v}{\epsilon_r \epsilon_0 \dot{i}}$$

Where  $\mu$  is the dynamic viscosity of the electrolyte solution (Pa·s),  $\epsilon_r$  is the relative dielectric permittivity,  $\epsilon_0$  is the dielectric permittivity of vacuum,  $v$  is the horizontal velocity of bubble (m/s),  $K$  is the measured electrolyte conductivity (S/m), and  $A$  is the cross-sectional area of the electrophoretic unit (m<sup>2</sup>). Microscopic focusing on the stationary level in the cell correctly measures the zeta potential of bubbles.

An online particle counter (OPC Chemtrac System Inc., Model: PC 2400D-Laser Trac™, USA) was used to determine the size of the generated bubbles (see Figure 2.2).

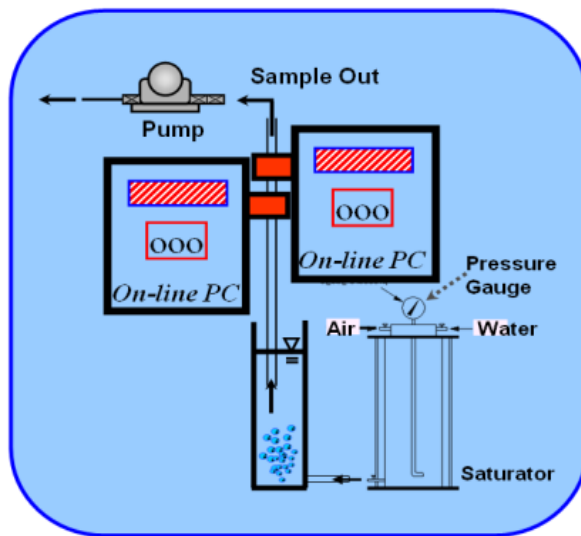


**Figure 2.2:** Schematic diagram of online particle counting method

The particle counter measured the size and the number of particles in accordance with the change in light intensity which was reflected by the particles or bubbles passing through the measurement cell and making the pulses. The number of pulses was the number of particles or bubbles and the height of pulses showed the particles or bubbles size. The size range of OPC

using in this case was from 2 $\mu$ m to 90  $\mu$ m, the flow-rate passing through the measurement cell was 100 ml/min with the interval time of 1 minute.

### 2.2.2. Bubble's zeta potential and size distribution

Bubble size and charge are one of the most essential characteristics that affect removal mechanisms. By adding coagulant (as Al<sup>3+</sup>), bubble's charge changed from negative (-29 mV of zeta potential) to positive (above +25 mV) (Figure 2.2), however positivity of bubble was not increased any more at above 5 mg/L of coagulant, staying at 26~29 mV. This characteristic concerns with modelling of collision between bubble and particles so that positively charged bubble appreciate attaches greatly with negatively charged flocs cell, enhancing removal efficiency of flotation process.

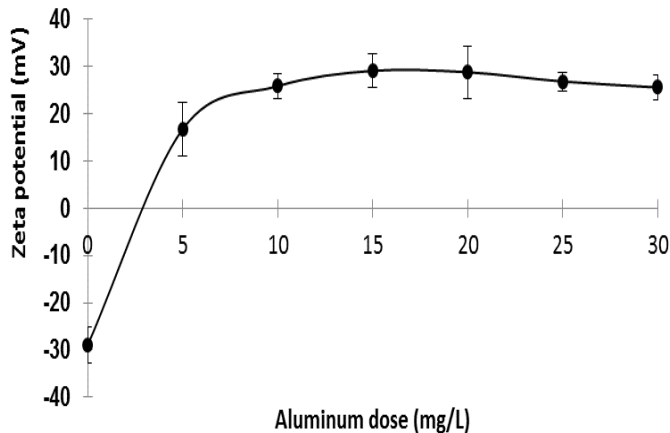


**Figure 2.3:** Zeta potential of bubble in various coagulant dose.

The generation of positively charged bubbles was also reported in a previous study, provided in Figure 2.3 (Han, 2006). As seen in Fig. 2.3, the

bubble zeta potential was positive in the presence of  $10^{-2}$  M  $\text{Al}^{3+}$  at pH 2–8.2 with a maximum of +30 mV;  $10^{-2}$  M magnesium ( $\text{Mg}^{2+}$ , a divalent metal ion) at pH 9 yielded a maximum of +15 mV. Other metal ions such as  $\text{Na}^+$ ,  $\text{K}^+$ , and  $\text{Ca}^{2+}$  yielded negative zeta potentials at pH 2~13 (Fig. 2.4). Thus, cationic covalent metals are rapidly adsorbed onto the bubbles, creating positive electric potential at the interface. In this study, zeta potential influenced the removal efficiency of filamentous algae by the bubble flotation method.

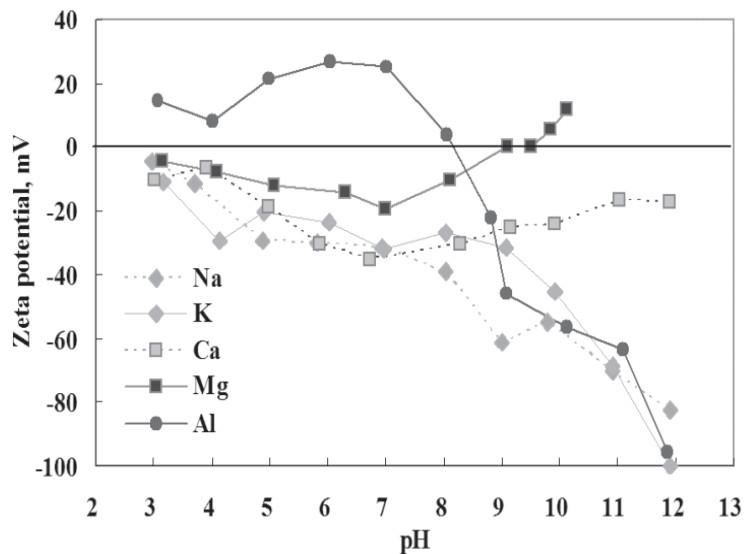


**Figure 2.4:** Bubble zeta potential in the presence of metal solutions (by Han and Dockko, 2004).

At higher saturated pressure, bubble size decreased; at a critical pressure of ~3.5 bars, the average bubble size was constant (Han, 2002; Kim, 2012). Previous reports suggest average bubble sizes of 28  $\mu\text{m}$  at critical pressure

and  $>40 \mu\text{m}$  at lower pressures (Han, 2002). Similar results were reported elsewhere (De Rijik, 1994; Hudson, 2009); however, bubble size in this study reached  $30 \mu\text{m}$  at 6 bars and  $45 \mu\text{m}$  at 3 bars when the bubble rate was fixed at 30% (see Table 2.1). Our average bubble size was slightly larger than those reported by Han (Han, 2002).

**Table 2.1**

Average bubble size and pressure

Pressure (bars)	Size range ( $\mu\text{m}$ )	Average size ( $\mu\text{m}$ )	References
6	10–90	30	In this study
	15–85	28	Han <i>et al.</i> (2002)
3	10–110	45	In this study
	15–85	41	Han <i>et al.</i> (2002)

This can be explained by the possible coalescence or overlapping of bubbles during their transport to the tube and sensor of the OPC. In addition, the bubbles inside the tube and sensor of the OPC cannot collapse to form smaller bubbles, and the opportunity for bubble coalescence might rise with the increase in transport duration from the reactor to the sensor of OPC.

Since the collision between similar size of bubbles and particle will enhance removals, thus these bubble size might be potential effective to remove with algae species in this study.

### 2.3. Batch testing

Bubbles generated from a saturator were injected to an acrylic-made cylindrical reactor with algae-containing water (Figure 2.5).

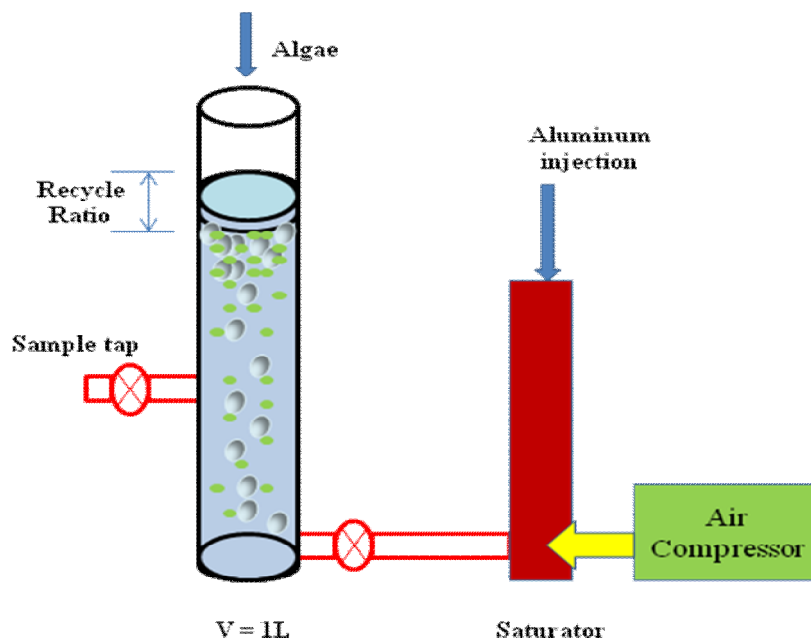


**Figure 2.5:** Schematic diagram of algae removal by Batch DAF

Batch type DAF experiments were performed at a room temperature ( $25 \pm 1^\circ C$ ) with added  $Al^{3+}$  ( $0 \sim 30$  mg/L with an increment of 5) and batch-type flotation with bubbles of varying concentration, charge, and size. The

separation time of BDAF was 3~5 mins. At the end of flotation process, samples were collected to investigate removal efficiency (cell number and chlorophyll *a* concentration), and changes in algal morphology were observed by microscopy (Sometech, Korea) and image analysis.

## REFERENCES

Han MY, Kim, M. K., Ahn, H. J. 2006. Effects of surface charge, micro-bubble size and particle size on removal efficiency of electro-flotation. *Water Science and Technology* 53(7):127-132.

Han M. Y. KMK, Shin M. S. 2006. Generation of a positively charged bubble and its possible mechanism of formation. *Journal of Water Supply: Research and Technology - AQUA* 55(7 - 8):471 - 478.

Han MY, Kim, W., Dockko, S. 2001b. Collision efficiency factor of bubble and particle ( $\alpha_{bp}$ ) in DAF: theory and experimental verification. *Water Science and Technology* 43(8):139-144.

Han MY, Dockko, S. 1998. Zeta potential measurement of bubbles in DAF process and its effect on removal efficiency. *KSCE Journal of Civil Engineering* 2(No 4):461-466.

Hudson JBC, Daniel G. N., Reiner N., Sílvia C.A. F. 2009. Micro-bubble size distribution measurement by laser diffraction technique. *Minerals Engineering* 22:330 - 335.

Kim TI, Kim, Y. H., Han, M. Y. 2012. Development of novel oil washing process using bubble potential energy. *Marine Pollution Bulletin* 64(11):2325-2332.

De Rijik, S.E., Van Der Graaf, H. J. M., Den Blanken, J. G., Bubble size in flotation thickening. *Water Reasearch*, 1994. 28(2): p. 465 - 473.

# Chapter 3. REMOVAL OF DIFFERING ALGAL SHAPES BY CHARGED BUBBLE FLOTATION

## 3.1. Introduction

In freshwater basin, although many algal species develop simultaneously but they are formed in some common shape such as spherical, oval (as known as spherical-like), filamentous and so on (Sze, 1998). Characteristics of algae affecting treatment efficiency are morphology, motility, surface charge, cell density and the extracellular organic matter (EOM) composition, the number of cell or concentration of chlorophyll a (Henderson *et al.*, 2008). It's demonstrated that at natural conditions, algae are negatively charged therefore it requires positive bubbles for higher removal efficiency (Han *et al.*, 2001; Henderson *et al.*, 2010). When employing positive bubble generated from a saturation pressure of 6 bars with covalent metal ion as a coagulant, higher removal efficiency was obtained compared to the conventional DAF process (Malley, 1995). Morphology of algae including shape and size may have impacts on the performance of flotation process when considering the bubble-cell attachment, in addition, algae removals are also dependent on algal species (Jarvis *et al.*, 2009; Teixeira *et al.*, 2010). Thus, this chapter compares the removal efficiencies of differing algal shapes by bubble technology. In

particular, the aims of this chapter are 1) to assess effect of algal shape (spherical, oval and filamentous shape, represented by *Microcystis sp.*, *Chlamydomonas angulosa* and *Phormidium sp.*, respectively) on flotation performance and 2) to compare the optimum dose of coagulant adding to achieve the best removal efficiencies of differing shape of algae.

### **3.2. Materials and method**

#### **3.2.1. Algal culturing**

Three algae species in this work were obtained from the Korean Marine Microalgae Culture Center (KMMCC), Busan, South Korea shown as follows:

- 1) *Microcystis sp.* (KMMCC #1517), sampled at Lake Paldang, South Korea – a green algae;
- 2) *Chlamydomonas angulosa* (KMMCC #866), sampled at Upo, South Korea – a green algae; and
- 3) *Phormidium sp.* (KMMCC #1218), sampled at Upo, South Korea – a green algae.

Three algae species were cultivated in the same condition of Jaworski's Media (see Table 3.1), growth temperature of 20°C, a salinity of 0‰, a brightness throughput of 2,000 lux, a lighting cycle of 10-hr lights/ 14-hr dark. The culture was shaken at 150 rpm for 20 days. This culture regime was intended to mimic the optimal growth conditions of algae in nature.

**Table 3.1.**

Composition of JM (Javorski's Medium)

Order	Compounds	Concentration (per 200 mL)
1	Ca (NO <sub>3</sub> ) <sub>2</sub> . 4 H <sub>2</sub> O	4.0 g
2	KH <sub>2</sub> PO <sub>4</sub>	2.48 g
3	MgSO <sub>4</sub> . 7 H <sub>2</sub> O	10.0 g
4	NaHCO <sub>3</sub>	3.18 g
5	EDTAFeNa	0.45 g
	EDTANa <sub>2</sub>	0.45 g
6	H <sub>3</sub> BO <sub>3</sub>	0.496 g
	MnCl <sub>2</sub> . 4H <sub>2</sub> O	0.278 g
	(NH <sub>4</sub> ) <sub>6</sub> Mo <sub>7</sub> O <sub>24</sub> . 4 H <sub>2</sub> O	0.20 g
7	Cyanocobalamin	0.008 g
	Thiamine HCl	0.008 g
	Biotin	0.008 g
8	NaNO <sub>3</sub>	16.0 g
9	Na <sub>2</sub> HPO <sub>4</sub> . 12 H <sub>2</sub> O	7.2 g

Algae characteristics were addressed in term of shape, size, number of cells and their surface charge. The shape of algae was identified with a microscope (Somotech, Korea) and the growth rate under cultivated condition was monitored as the number of cell and the concentration of

chlorophyll a. The number of algae was determined using cell counting with a haemocytometer and its numbers in this study were found to at  $6.5 \times 10^6 \pm 2 \times 10^5$  cells/L (initial cell numbers when they were injected to DAF-cylindrical reactor). Measurement of chlorophyll a was conducted in accordance with the Standard Methods (APHA; AWWA; WPCF, 1998 #23). The size distribution of algae was obtained from the online particle counter (Chemtrac System Inc., Model: PC 2400D-Laser Trac™, USA), as provide in Fig. 2.4. Zeta potentials at pH 4–7 were measured with a zetaphotometer (ALPHAPHOT – 2, SY2, France), and pH was adjusted with  $\text{NaH}_2\text{PO}_4/\text{Na}_2\text{HPO}_4$  and  $\text{CH}_3\text{COOH}/\text{NaCH}_3\text{COO}$ .

### 3.2.2. Experimental setup

The BDAF testing for algal removal was mentioned in chapter 2 (see section 2.3). The total of series BDAF testing is summarized in Table 3.2 as followings

**Table 3.2**

BDAF tests for removal of differing algal shapes

Bubble generation	Testing
Bubble injection: 30%	Spherical algae: T1 ~ T7
Coagulant: aluminum 0~ 30 mg/L	Oval algae: T8 ~ T14
Pressure: 6 bars	Filamentous algae: T15 ~ T21

### 3.3. Results and discussion

#### 3.3.1. Algal properties

Under cultivated conditions, three algae species were identified in different shapes (shown in Figure 3.1-a, with photographs). As seen, *Microcystis sp.* had spherical shape, and the shape of *Chlamydomonas angulosa* was oval, consisting of unicellular flagellates. *Phormidium sp.* was in filamentous shape with several segments, in which each could be considered as one single cell.



**Figure 3.1:** The shape of three algal species under cultivated condition

In terms of size distribution, it was found that almost all of spherical algae present below 8  $\mu\text{m}$ , showing that more than 50% of algae were less than 6  $\mu\text{m}$  size. Meanwhile, the majority of oval and filamentous algae were in the range of 6~12  $\mu\text{m}$  which were a little bit larger than spherical algae, and their sizes were widely distributed up to ~20  $\mu\text{m}$ . The only noticeable difference between these two algae was that oval algae, in the vicinity of 8  $\mu\text{m}$ , was likely to show more dominant and mono-dispersed distribution

rather than filamentous algae (Figure 3.2).

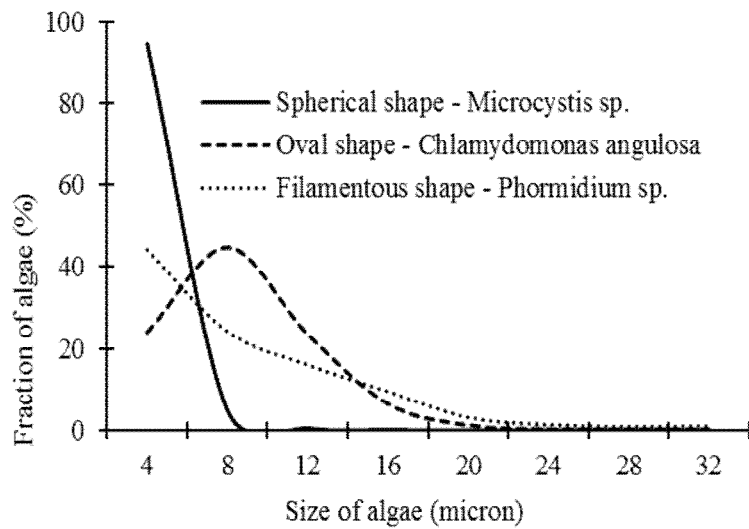


**Figure 3.2:** Initial size distribution of three algal species

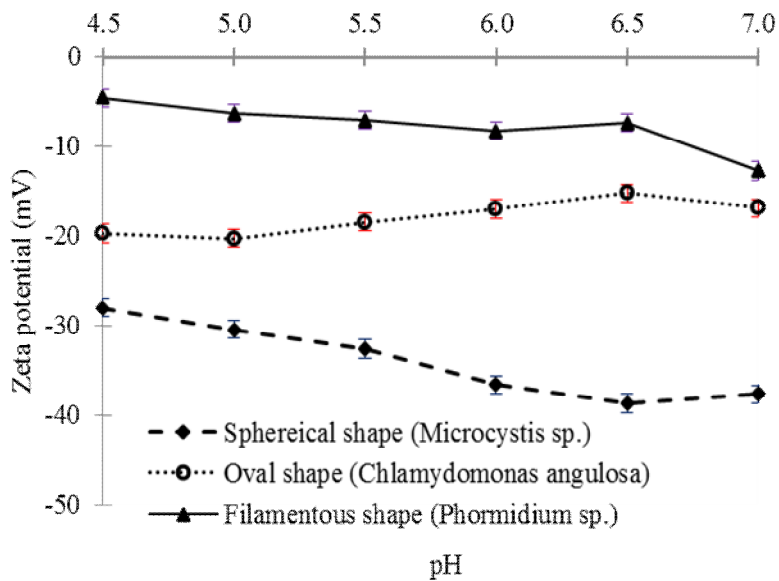


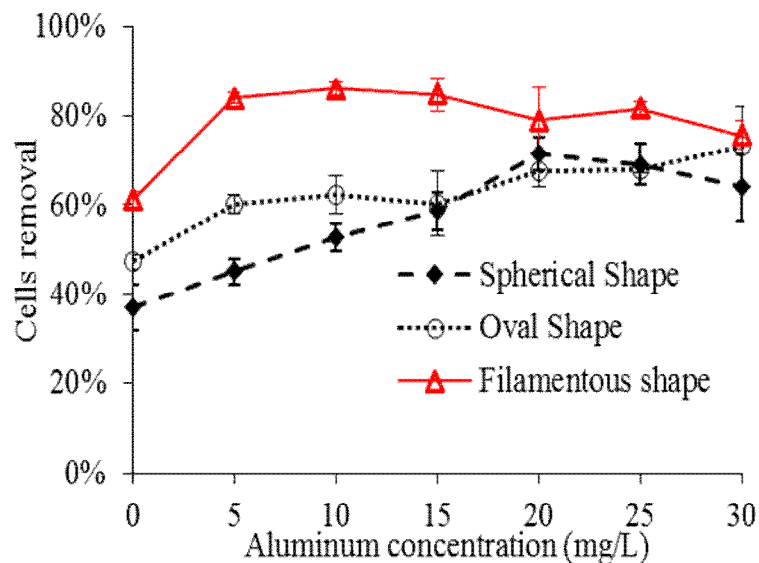
**Figure 3.3:** Zeta potential of three algal shapes

In the range of pH from 4.5 to 7.0, zeta potential of algae was negative regardless of its shape (Figure 3.3). Zeta potential was the lowest for filamentous algae and the highest for spherical alga; ~ -10 mV and ~ -40 mV, respectively, however, the values for both algae slightly decreased as pHs decreased. Zeta potential of oval algae varied slightly from -22 mV to -16 mV when increasing pH. In this work, pH had more impacts to the charge of spherical and filamentous species than of oval specie. Since they charged the negatively, it may imply that positive bubbles potentially get the high removal efficiency.

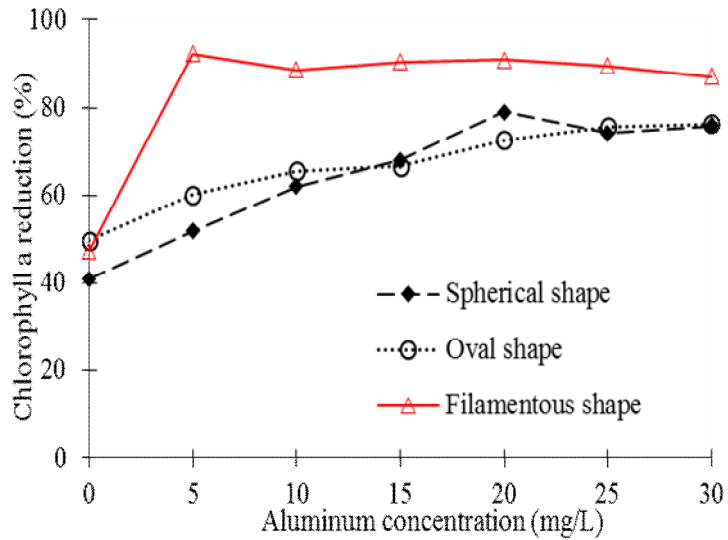
### **3.3.2. Removal efficiencies**

Figure 3.4 indicates removal efficiencies based on the number of cells, which is one of the most important parameters for assessment algae removal. As seen in the figure, positively charged bubbles were more effective on removal efficiency, expressed more obviously by number of cells than by chlorophyll *a*, enhancing from 8% to 23% for spherical shape, 6% to 14% for oval shape and 23% up to 44% for filamentous shape. For chlorophyll *a*, removal tendency was similar to the cell removal (see Fig. 3.5). Because bubbles with coagulant charged positively and during the experimental period, zeta potential of these algae were negative therefore the efficiency enhancement was the certain results.

Prominently, filamentous algae presented the best and the most stable result. At 5 mg/L of  $Al^{3+}$ , the highest efficiency was obtained, showing by ~86% for the cell removal and ~94% for chlorophyll *a* then it slightly decreased regardless of increase of  $Al^{3+}$ . In general, performance of oval (spherical-like) algae trended upwardly in perspective of adding more aluminum. At the same operational conditions, spherically-shaped algae presented the unstable results. The impacts of coagulant doses to spherical and oval (spherical-like) shape are clearer than filamentous configure. *Microcystis sp.* (spherical structure) was gradually enhanced at ~20 mg/L while *Chlamydomonas angulosa* was continuously increased in the range of applied coagulant doses (5~30 mg/L).



**Figure 3.4:** Cell removals of differing algal shapes



**Figure 3.5:** Chlorophyll *a* reduction of differing algal shapes

Although the size of spherical algae seems to aid better result than other shapes but in fact, the number of cells was removed in reverse order as filamentous > oval > spherical algae. The reason for this phenomenon is the collision mechanism by zeta potential of algae and bubble. Although all of differing algae species charge negatively at the experimental conditions but filamentous shape with lower negatively ZP ( $\sim -10$  mV) would have more chance to collide with bubbles (ZP:  $\sim +25$  mV) than spherical and oval algae ( $\sim -20$  to  $-40$  mV). At this point, *Phormidium sp.* will consume less energy so that they easily floated to surface in a short time. On the other hand, *Chlamydomonas* is shaped in ovally, consists of two equal flagella which swim by breast-stroking therefore their cells can rotate while swimming in order to enhance the collision with bubbles. View from these

points, *Microcystis sp.* were in the stress situation for enhancement separation of micro-bubble process.

### **3.4. Summary**

This chapter compared removals of differing algal shapes by flotation process. At the bubble rate of 30%, filamentous algae required the least aluminium concentration (only 5 m/L) and the greatest removal (i.e. ~88% for cell removal and ~94% for chlorophyll *a* reduction). The results could be attributed to the difference of algal zeta potential values on collision mechanism between algae and bubble, in which filamentous algae with the lowest negativity of zeta potential (in comparison with spherical and spherical-like algae) consumed less energy from positively charged bubble to divide their cells. In addition, this chapter also indicates some information about potential effects of algal shape on their treatability by charged bubble flotation that will be discussed more deeply in the consequent chapters of this study.

## REFERENCES

Henderson, R., Parsons, S. A., Jefferson, B., The impact of algal properties and pre-oxidation on solid-liquid separation of algae. *Water Research*, 2008. 42(8-9): p. 1827-45.

Han, M., Kim, W., Dockko, S., Collision efficiency factor of bubble and particle ( $\alpha_{bp}$ ) in DAF: theory and experimental verification. *Water Science and Technology*, 2001. 43(8): p. 139-144.

Henderson, R.K., Parsons, S. A., Jefferson, B., The impact of differing cell and algogenic organic matter (AOM) characteristics on the coagulation and flotation of algae. *Water Research*, 2010. 44(12): p. 3617-24.

Malley, J.P., The use of selective and direct DAF for removal of particulate contaminant in drinking water treatment. *Water Science and Technology*, 1995. 31: p. 49-57.

Sze P. 1998. *A Biology of the Algae*. Margaret J. Kemp KRL, editor: Michael D. Lange.

Teixeira, M.R., Sousa, V., Rosa, M. J., Investigating dissolved air flotation performance with cyanobacterial cells and filaments. *Water Research*, 2010. 44(11): p. 3337-44.

## Chapter 4. OPTIMAL CONDITION FOR BETTER REMOVAL OF FILAMENTOUS ALGAE

### 4.1. Introduction

Among the chain-like filamentous algae, *Phormidium* sp. is the one of the most common species in floating mats on the water surface (Hilda Canter-Lund and WG-Lund, 1996; Sze, 1998). This algal nuisance reduces water quality and causes the filter bed to become clogged in conventional water treatment plants (Bauer M. J. and others, 1998; Graham N. J. D. and others, 1998; Hargenshainer E. E. and Watson S. B., 1996). Maintaining negative to low positive zeta potential is key to successful algal removal, especially for spherical or spheroid cells (Henderson, 2008b; Henderson, 2010; Taki and others, 2008). Similar sized bubbles increase collisions of the bubble–particle attachment, thus improving removal efficiency (Han, 2001b); however, there have been few studies on the collision mechanism of bubbles and filamentous cell aggregates and optimal tools for removal of filamentous algae. By comparing removals of filamentous algae with spherical and/or spherical-like algae, this chapter aimed to optimized bubble formation by determining the ideal concentration (amount of bubbles

injected), zeta potential (by adding dosed coagulants), and bubble size (by changing saturating pressures) for removal of *Phormidium* sp. and chlorophyll *a* reduction.

## **4.2. Materials and Methods**

### **4.2.1. Phormidium sp. culture and its properties**

*Phormidium* sp., a representative chain-like algae, was purchased from Korea Marine Microalgae Culture Center (KMMCC #1218, sampled from Upo, South Korea swamp surface water) and cultured in the laboratory (see 3.2.1 section – chapter 3).

### **4.2.2. Bubble generation and batch testing**

For better removal of filamentous algae, charged bubble flotation was conducted in various conditions, such as the differences of zeta potential values, sizes and bubble rates injected to the reactor. Bubble concentration was controlled by changing the injection amount (10%, 20%, and 30%), and size was modulated by changing the pressure (3 bars and 6 bars). Zeta potential was controlled by adding various concentrations of  $\text{Al}^{3+}$  (0, 0.5, 1, and 5 mg/L). These experiments are summarized in Table 4.1.

**Table 4.1**

Summary of experimental conditions for better removal

Set 1: Change of bubble rate	Set 2: Change of pressure
Bubble rates: 10%, 20%, 30%	Bubble rate: 30%
Pressure: 6 bars.	Pressure: 6 bars, 3 bars
Coagulant: Al <sup>3+</sup> : 0, 0.5, 1, 5 mg/L	Coagulant: Al <sup>3+</sup> : 0, 0.5, 1, 5 mg/L

### 4.3. Experimental results

#### 4.3.1. Characteristics of *Phormidium* sp.

The morphology of *Phormidium* sp. under cultivated conditions is provided in Table 4.2 with an image. *Phormidium* sp. is a chain-like alga with cells formed in segments, each of which is spheroid. Most of the segments are surrounded by a continuous cuticle to form the filament. These chain-like cells range from 2 to 10  $\mu\text{m}$  in diameter and about 100 to 200  $\mu\text{m}$  in length (see in Table 4.2).

Acidic pH (4.0–7.0) yielded negative zeta potentials (Fig. 4.3). The zeta potential of *Phormidium* sp. changed from -4 mV to -12 mV with increasing pH, thus demonstrating the minimal effect of pH on zeta potential.

**Table 4.2**

Morphology of *Phormidium* sp. cultivated in flasks and the concentration used for flotation experiments

Shape	Image	Size	Experimental concentration	
			Cell counting (cells/mL)	Chl- <i>a</i> mg/m <sup>3</sup>
Chain-like		Diameter: 2–10 μm Length: 100–200 μm	2,000 ± 50	58.46

### 4.3.2. Removal efficiencies

#### 4.3.2.1. Effects of the zeta potential of the bubble

Bubble zeta potential changed from negative to positive with the addition of Al<sup>3+</sup> (Fig. 4.1). Without coagulant, the zeta potential was -30 mV; with 1 mg/L and 5 mg/L Al<sup>3+</sup>, zeta potentials were +16 mV and +27 mV, respectively. At 0.5 mg/L Al<sup>3+</sup>, the zeta potential was neutral (Fig. 4.1).

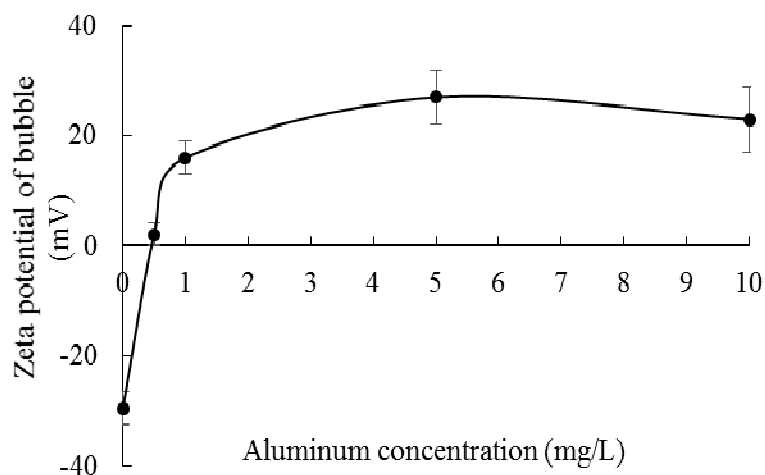


**Figure 4.1:** Bubble zeta potential in the presence of aluminum ( $\text{Al}^{3+}$ ).

Bubble zeta potential influences the efficiency of *Phormidium* sp. removal (Fig. 4.2). Positively charged bubbles enhanced removal efficiencies better than negatively charged bubbles did. Better removal efficiencies were obtained with more strongly positive bubbles, probably because of the overall negative charge of the *Phormidium* sp. cells. Optimal removal of cells (88.24%) was observed at a zeta potential of approximately +20 mV; removal of chlorophyll *a* (~94%) required a bubble zeta potential of +27 mV; these removal rates were observed with 1 mg/L and 5 mg/L  $\text{Al}^{3+}$ , respectively. These high removal rates can be explained by the relative positivity of zeta potential observed due to the coagulant concentration (5 mg/L  $\text{Al}^{3+}$ ), which helped break up the chain-like cells more effectively than a concentration of 1 mg/L. This would mean that even at higher cell removal, lower chlorophyll *a* reduction could occur.

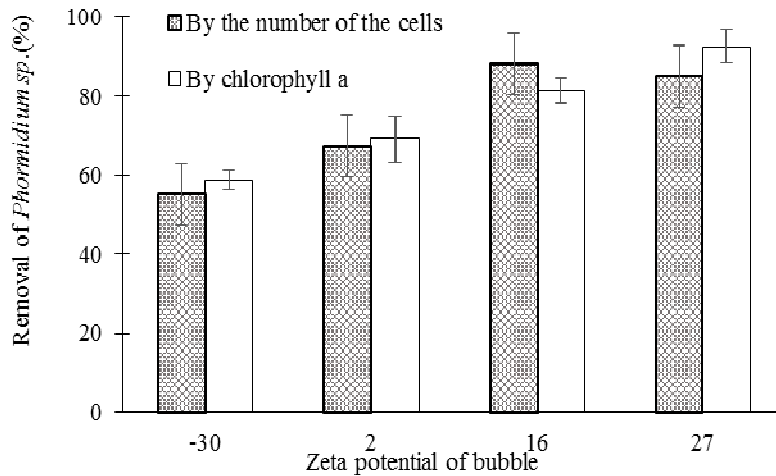


**Figure 4.2:** *Phormidium* sp. removal by flotation method

Mobility shift assays demonstrated the changing zeta potential of *Phormidium* sp. after they were broken by the bubble flotation method (see Table 4.3). At pH 4–7, the overall negativity of these shorter cells shifted from -12.92 mV to -30.09 mV, except at pH of 4.5 with -10.82 mV (see Figure 4.3).

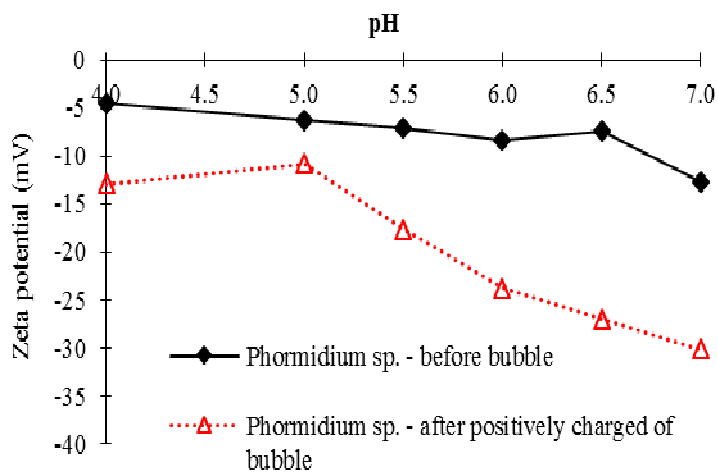


**Figure 4.3:** Zeta potential of *Phormidium* sp. in flotation process.

The zeta potentials of the shorter cells were much higher than the initial zeta potentials (zeta potential at pH 6.5 was -7.35 mV for the original filamentous cells and -26.98 mV for the shorter chain-like cells).

**Table 4.3**

Mobility of *Phormidium* sp. before and after positively charged bubble flotation

pH	Before		After	
	Mobility ( $\mu\text{m/s/V/cm}$ )	Standard deviation	Mobility ( $\mu\text{m/s/V/cm}$ )	Standard deviation
4.0	-0.36	0.12	-1.02	0.04
5.0	-0.50	0.16	-0.85	0.01
5.5	-0.56	0.20	-1.39	0.09
6.0	-0.65	0.14	-1.87	0.21
6.5	-0.58	0.03	-2.12	0.13
7.0	-1.00	0.12	-2.34	0.53

The length of the chain-like cells likely affected their mobility at varying pH; longer cells were less mobile and exhibited a smaller negative zeta potential. Positively charged bubbles broke the long chain-like cells into shorter chains, explaining the change of zeta potentials of the newly

generated shorter cells after positive bubble flotation.

#### 4.4.2. The effects of bubble size

Bubble size affected cell and chlorophyll *a* removal (Fig. 4.4 and Fig. 4.5). At a 30% bubble injection rate, 30- $\mu\text{m}$  bubbles (formed at 6 bars) provided greater removal efficiencies (~85% for cells and ~93% for chlorophyll *a*) than the 45- $\mu\text{m}$  bubbles (formed at 3 bars; ~73% cell removal and ~82% chlorophyll *a* reduction).

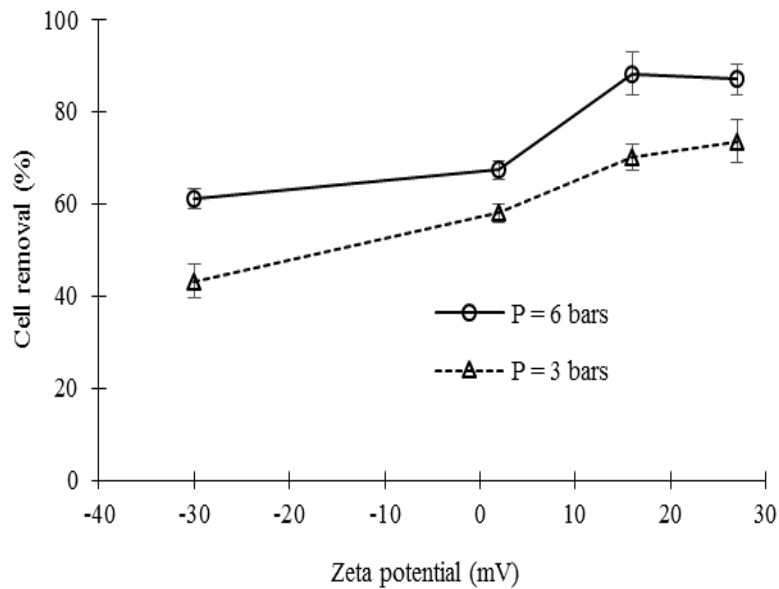


**Figure 4.4:** Cell removal of *Phormidium* sp. with different bubble sizes.

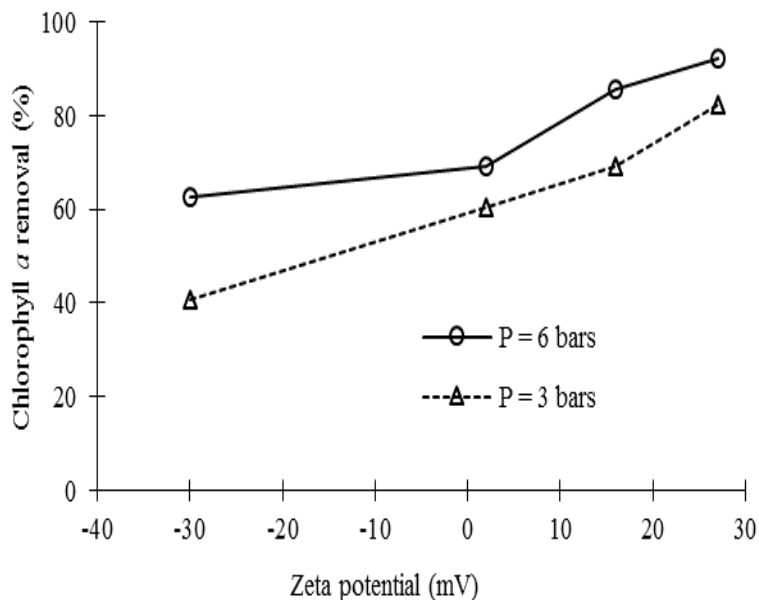


**Figure 4.5:** Chlorophyll *a* reduction of *Phormidium* sp. with different bubble sizes.

This result was attributed to the different bubble sizes generated for the treatment process and to the relatively small size of *Phormidium* sp. cells, which are 2–10  $\mu\text{m}$  wide and about 100–200  $\mu\text{m}$  long. Moreover, it can be also interpreted that with the chain-like cells, the collision targeting the diameter could be more frequent than that targeting the length; thus, the smaller bubble would collide and aggregate more greatly with filament. In other words, better attachment would occur with a 30- $\mu\text{m}$  bubble rather than a 45- $\mu\text{m}$  one.

#### 4.4.3. The effects of bubble concentration

*Phormidium* sp. separation efficiencies varied with bubble concentration. In particular, the decreasing order of removal was 30% > 20% > 10%. Negatively charged bubbles provided the least efficient cell removal at all bubble injection rates. Cell removal did not significantly differ between 20% and 30% bubble injections, both providing ~60% removal. Adding 5 mg/L of Al<sup>3+</sup> enhanced cell removal, with optimal results at all bubble rates (Fig. 4.6). We observed similar results for chlorophyll *a* (Fig. 4.7). However, optimal chlorophyll *a* removal of up to 93% was achieved compared to 86% cell removal at 30% bubble concentration with a zeta potential of +27 mV.

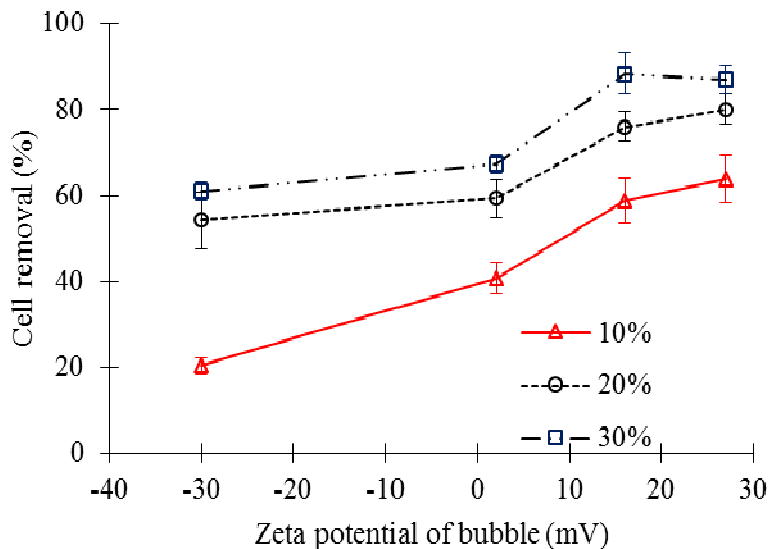


**Figure 4.6:** Cell removal of *Phormidium* sp. at different bubble rates.

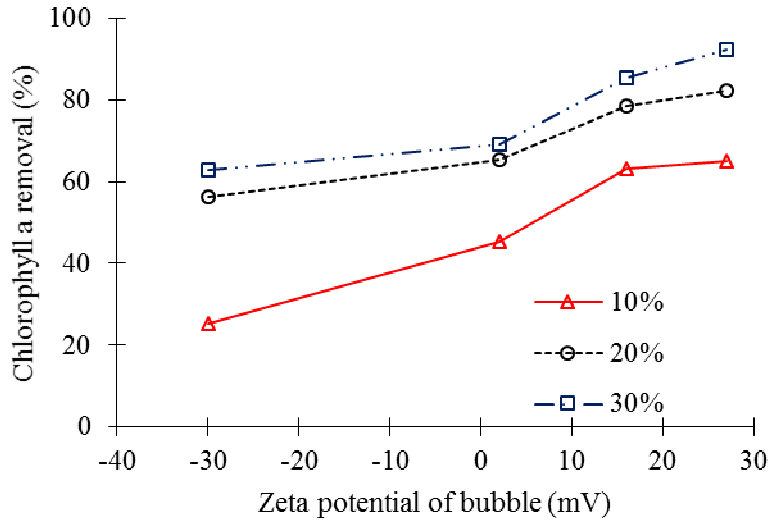


**Figure 4.7:** Chlorophyll *a* reduction of *Phormidium* sp. at different bubble rates.

We found that application of more bubbles increased the frequency of bubble–algae aggregates and thus removal of more *Phormidium* sp. to the surface. However, at the highest bubble concentration, chlorophyll *a* removal was substantially more efficient than cell removal. Since the chain-like filaments are easily divided into smaller segments that may float to the surface or stay in the water, depending on the bubble injection concentration. In this case, the optimum amount of bubbles to attach and shear strain cells was at 30% bubble concentration. Moreover, segments that remain in the water are counted as new cells, but they are smaller and contain much less chlorophyll *a* content than the initial filament. Thus, it appears that more chlorophyll *a* was removed at 30% bubble rate, and at

lower bubble rates, chlorophyll *a* reduction was at par with a reduction in the number of cells.

#### **4.4. Summary**

In this chapter, *Phormidium* sp. removal was attempted by flocculation and by charged bubble flotation. We found that positively charged bubbles provided the most efficient algal removal. We surmise that collision of positive bubbles and filamentous cells occurs via breakup of the chain-like cells and attachment of the detached shorter algae to the bubbles, which then float to the surface. In addition, the *Phormidium* sp. chains become smaller and spheroid. Thus, bubble-generating conditions influence the removal and morphology of *Phormidium* sp. Optimal results were obtained with a 30% bubble injection rate and 30- $\mu\text{m}$  bubble size, with a zeta potential range of +16 mV to +27 mV, in the presence of 5 mg/L  $\text{Al}^{3+}$ . We conclude that positively charged bubble flotation is a viable method for filamentous algal removal in freshwater.

## REFERENCES

Bauer M. J., Barley R., Chipps M. J., Eades A., Scriven R. J., J. RA. 1998. Enhanced rapid gravity filtration and dissolved air flotation for pre-treatment of river Thames reservoir water. *Water Science and Technology* 37:35 - 42.

Graham N. J. D., Wadrdlaw V. E., Perry R., al. e. 1998. The significance of algae as trihalomethane precursors. *Water Science and Technology* 37(2):83 - 89.

Han MY, Kim, W., Dockko, S. 2001b. Collision efficiency factor of bubble and particle ( $\alpha_{bp}$ ) in DAF: theory and experimental verification. *Water Science and Technology* 43(8):139-144.

Hargenshainer E. E., Watson S. B. 1996. Drinking water treatment options for taste and odor control. *Water Reasearch* 30(6):1423 - 1430.

Henderson RK, Parsons, S. A., Jefferson, B. 2008b. Successful Removal of Algae through the control of Zeta potential. *Separation Science and Technology* 43(7):1653 - 1666.

Henderson RK, Parsons, S. A., Jefferson, B. 2010. The impact of differing cell and algogenic organic matter (AOM) characteristics on the coagulation and flotation of algae. *Water Research* 44(12):3617-3624.

Hilda Canter-Lund, WG-Lund J. 1996. *Freshwater Algae: their microscopic world explored*: Biopress Ltd.

Phoochinda W, White, D. A. 2003. Removal of algae using froth flotation. *Environmental Technology* 24(1):87-96.

Sze P. 1998. *A Biology of the Algae*. Margaret J. Kemp KRL, editor: Michael D. Lange.

Taki, K., Seki, T., Mononobe, S., Kato, K., Zeta potential measurement on the surface of blue-green algae particles for micro-bubble process. *Water Science and Technology*, 2008. 57(1): p. 19-25.

## Chapter 5. THE CHANGE OF ALGAL MORPHOLOGY BY POSITIVELY CHARGED BUBBLE FLOTATION

### 5.1. Change of size distribution

Size distribution of algae species in this study did not depend on recycling ratio. Their sizes arrangements overall unchanged in some cases of bubble injecting to the reactor, governing from 2~6  $\mu\text{m}$  for *Microcystis sp.* – a spherical algae (Figure 5.1), below 15  $\mu\text{m}$  for *Chlamydomonas angulosa* – an oval algae (Figure 5.2) and below 20  $\mu\text{m}$  for *Phormidium sp.* – a representative of filamentous species (Figure 5.3). According to Fig. 5.1, spherical cell diameters were allocated identically as more than 93% of the cells sized from 2~6  $\mu\text{m}$  without regard to the accessions to bubbles of coagulant. Similarly, the flotation process with coagulant did not lead the change of optimum size range for oval shape, staying at below 15 $\mu\text{m}$  (Fig. 5.2). Furthermore, the fraction of cells was approximately ~20% from 2~6  $\mu\text{m}$ , ~50% from 6~10  $\mu\text{m}$  and ~25% from 10~14  $\mu\text{m}$  (Fig. 5.3). Interestingly, a big difference in the size distribution between bubble only and bubble with  $\text{Al}^{3+}$  tests occurred with *Phormidium sp.* – a filamentous algae. As seen in figure 5.3, filamentous cells were arranged mostly below 20  $\mu\text{m}$  with ~30% fraction of each range from 2~6  $\mu\text{m}$  and from 6~10  $\mu\text{m}$ , ~20% of 10~14  $\mu\text{m}$ , over 10% of 14~20  $\mu\text{m}$  when coagulant was absent.

Due to the impacts of aluminium, the proportion of 6~20  $\mu\text{m}$  cells were decreased by 40%, hence, the increase in the fraction of below 6  $\mu\text{m}$  cells had resulted in smaller cells' presence.

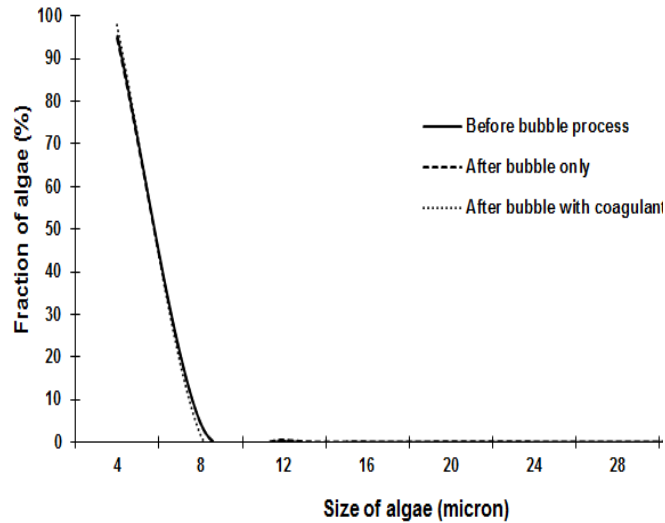


**Figure 5.1:** The change of the size distribution of spherical algae by flotation

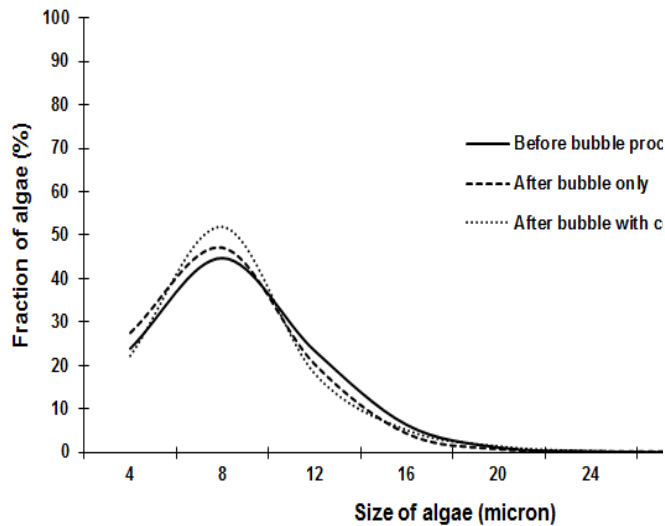


**Figure 5.2:** The change of the size distribution of oval algae by flotation

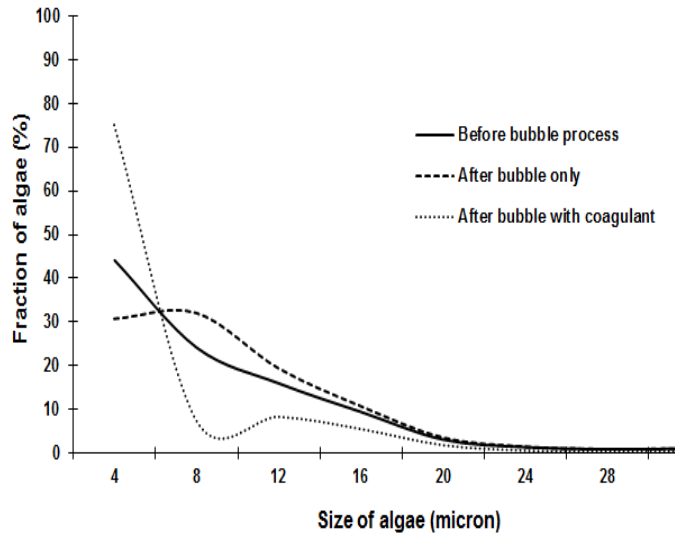


**Figure 5.3:** The change of the size distribution of filamentous algae by flotation

As discussed before, the filamentous algae would be easily divided or broken into its individual segments by external stress, and each segment can be identified as a sphere or oval, called spherical-segment and oval-segment. These configurations can keep their survival in lower pH environments, that is the reason for unchanged the size distribution of *Microcystis sp.* and *Chlamydomonas angulosa* at experimental conditions. Furthermore, the segments of *Phormidium sp.* would naturally shrink their diameters or release some their parts through the attachment with positive bubbles, produce the smaller sizes. The results, about 80% of below six-micron-cells of *Phormidium sp.* can be the reliable evidence to demonstrate the shape effect on size rearrangement of algae by flotation.

## 5.2. Change of algal shapes

The removal of three algae species in this study did show the different results and it was because of shape difference, i.e., spherical or so called spherical-like versus non spherical-like shape. On one hand, spherical-like algae would have higher feasibility to be floated as algae-bubble aggregates after colliding with certain amounts of bubbles, however, while filamentous algae might be difficult to be raised up to the surface with same amounts of bubbles, requiring more bubbles to be collide and attached to. Furthermore, it can be thought of possible releases of intra or extracellular organic materials from algae cell through collapsing bubbles onto or near algae, and subsequent cell-lysis occurred. Filamentous algae constituted with several segments would be vulnerable to such effects. Microscopic data provided somehow a different perspective about change of algae shape before and after applying bubble technology. Based on the changes of algae shapes/colour, the extraction of some contents inside the cells could occur. Because of the bubble with/without coagulant, singled spherical cells (*Microcystis sp.*) and oval cells (*Chlamydomonas angulosa*) unchanged their shapes but they likely colonized in the group (Figure 5.4).

Under the stress environment (pH = 4.5~6), filamentous cells (*Phormidium sp.*) adapted by dividing their length into segments where each segment would be oval in shape. Because the spherical structure is the strongest to be collapsed by turgor pressure (Wilcox, 2000) hence other

shapes would rather change their shape, near to spherical-shape as filamentous structure performed.

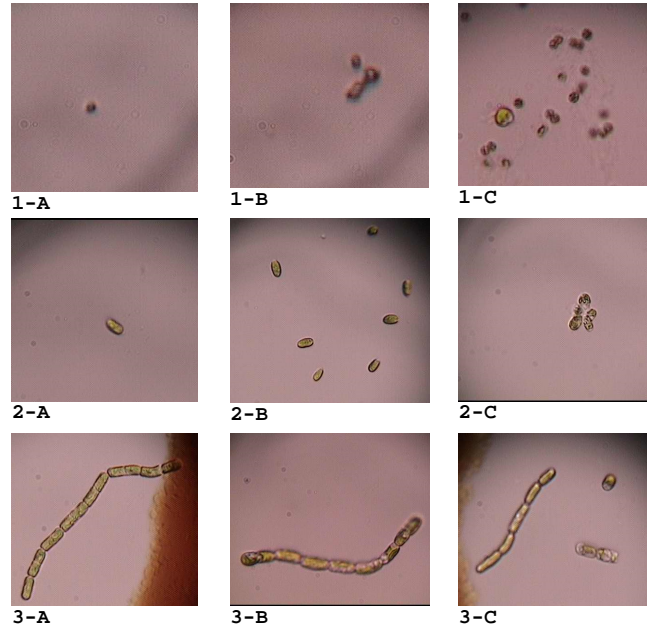


**Figure 5.4:** The change of algae shapes/color: Spherical shape – *Microcystis sp.* (1); Oval shape – *Chlamydomonas angulosa* (2);

Filamentous shape – *Phormidium sp.* (3). Observation conditions: Before bubble (A); After bubble only (B); After bubble with coagulant (C).

### 5.3. The breakup of filamentous algae and possible mechanism of removal

We characterized the changes in *Phormidium sp.* shape to investigate the mechanism by which positively charged bubble mediate cell breakup. In order to demonstrate the effect of positive bubbles on dividing *Phormidium*

sp. cells, we examined cell shape after flocculation and charged bubble flotation (Fig. 5.5). Flocculation and negatively charged bubble flotation did not break the chain-like shape of *Phormidium* sp.; thus, filament length was unchanged (see Fig. 5.5\_ a, b, c). Bubble flotation with added coagulant caused the chain-like cells to break at the cross walls of the segments (see Fig. 5.5\_d).

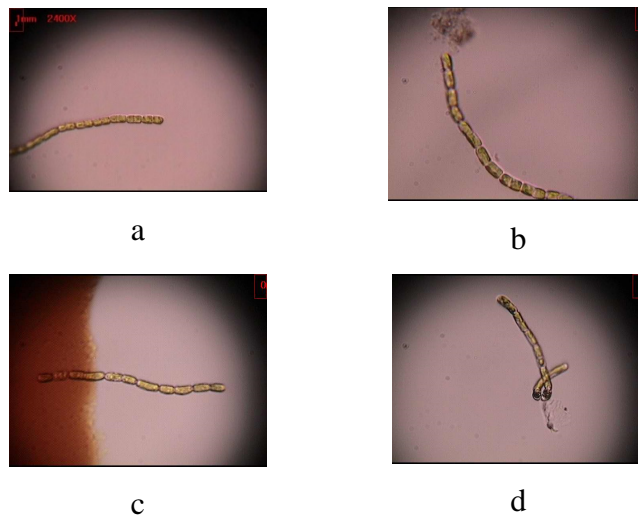


**Figure 5.5:** Microscopic images of broken cells: original shape (a), after coagulation (b), with negatively charged bubbles (c) and with positively charged bubbles (d).

Thus, only positive bubbles could shear the chain-like form. This breaking-off phenomenon could be attributed to the impact of the zeta potential on the collision of bubbles with the chain-like cells. As algal cells are negatively charged and the bubble zeta potential becomes positive with

coagulant addition, it is possible that the positive charge on the bubbles produces shear force that breaks the cell structure.

The only mechanism that led to chain breakup was flotation with positively charged bubbles. Figure 5.6 shows the possible mechanism of filamentous algal removal by positively charged bubbles. Filamentous algae were attracted to and quickly attached to the positively charged bubbles (see Fig. 5.6\_a). After a few seconds, the filamentous cells were broken, and the bubble–algae aggregate floated to the surface (Fig. 5.6\_b). Finally, at the end of the flotation process, *Phormidium* sp. took the form of shorter chains and spheroids.

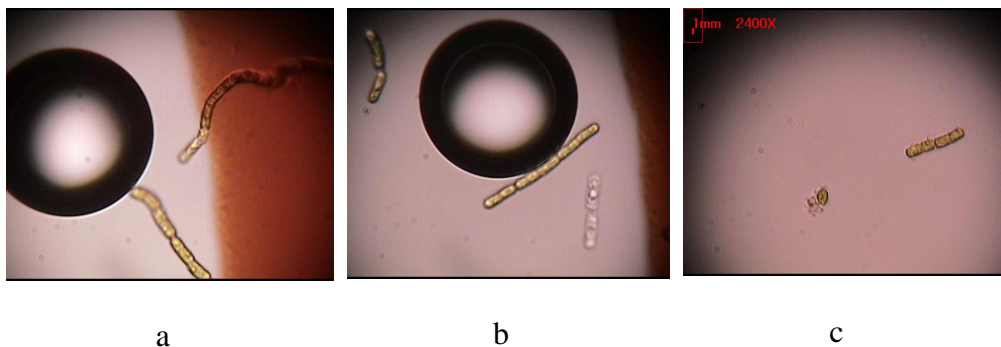


**Figure 5.6:** Collision of a *Phormidium* sp. filament and a positively charged bubble. The bubble attracted the negatively charged algae (a); bubble (~40  $\mu\text{m}$ ) attachment to algal filament (3.75  $\mu\text{m}$ ) and breakup (b); shorter algae after positively charged bubble (c).

Removal likely occurs via two steps: (1) chain-like cell breakup by positive bubbles and (2) simultaneous attachment of detached shorter algae and flotation to the surface. These two steps can be used for a higher removal efficiency of chlorophyll *a* in comparison to reduction in the number of the cells by positively charged bubble flotation.

The breakup mechanism occurs through the shear force of the bubble and the bonding force of the chain-like cell (Figure 5.7).

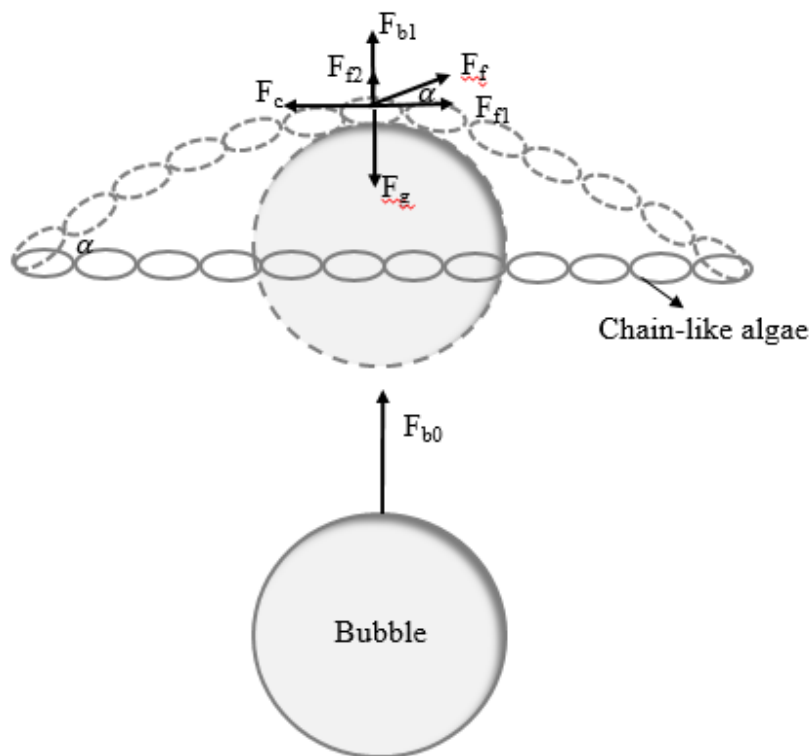


**Figure 5.7:** Net force exerted on the chain-like cells by the positively charged bubble

Assuming  $F_b$  is the net buoyant force, the shear force ( $F_{f1}$ ) can be calculated as follows:

$$\vec{F}_b = \vec{F}_{b1} + \vec{F}_f$$

Where  $F_{b1}$  ( $F_{b1} = F_b \cdot (1 - \sin^2\alpha)$ ) is the initial buoyant force of the bubble ( $F_{b0}$ ) and the body-force of the algae ( $F_g$ ), and  $F_f$  is the friction force caused by the interaction between bubble and algae ( $F_f = F_b \cdot \sin\alpha$ ).

The friction force  $F_f$  depends on the point of attachment between the bubble and algal filament; it is also a factor in the shear force ( $F_{f1} = F_b \cdot \sin\alpha \cdot \cos\alpha$ ) and buoyant force ( $F_{f2} = F_b \cdot \sin^2\alpha$ ). If the shear force ( $F_{f1}$ ) exceeds the net bonding force between the segments of the chain-like cells ( $\frac{1}{2} F_b \cdot \sin 2\alpha \geq \sum F_c$ ), the filament will break. At the angle  $\alpha$  of  $45^\circ$ , the shear force will reach the maximum magnitude of  $F_{b0}/2$ . In other words, the value of  $\alpha = 45^\circ$  is the ideal angle for breaking the chain-like cells with positively charged bubbles.

#### 5.4. Summary

This chapter investigated the change of morphology of three selected algal species during charged bubble flotation. The arrangement of algae size only presents the difference when filament algae (*Phormidium sp.*) was removed by bubble with coagulant, otherwise both spherical (*Microcystis sp.*) and oval algae (*Chlamydomonas angulosa*) unchanged their size

distribution in any perspectives of operational conditions. In the stress environment, spherical form is the strongest structure for the existence of cells hence filamentous one favours changing its shape, forming an oval structure which is very near to sphere to adapt to the living environment.

We surmised that collision of positive bubbles and filamentous cells occurs via breakup of the chain-like cells and attachment of the detached shorter algae to the bubbles, which then float to the surface. In addition, the *Phormidium* sp. chains become smaller and spheroid.

## Chapter 6. CONCLUSIONS

The conclusions of this study are as follow:

1. This paper compared removal efficiencies such as the number of the cells, chlorophyll *a* of differing algal shapes by charged bubble flotation. The bubbles in the absence and presence of aluminum in the range of 0 ~ 30 mg/L (with an increment of 5) were injected at 30% to remove three algal species. The results, increasing order cell removals and chlorophyll *a* was filamentous > spherical-like > spherical algae. The bubble with aluminum addition enhanced removals in all of three algal shapes, demonstrating that positively charged bubble is the better tool to remove algae in freshwater basin.
2. For filamentous algae (chain-like forming), the ideal operation conditions were investigated to achieve the best results. By accessing the effects of bubble zeta potentials, bubble's sizes and bubble rates, we found that at conditions with a 30% bubble injection rate and 30- $\mu\text{m}$  bubble size, with a zeta potential range of +16 mV to +27 mV, in the presence of 5 mg/L  $\text{Al}^{3+}$ , optimal removals of filamentous algae were obtained.
3. In this study, potential effects of algal shapes on their treatability by

charged bubble flotation (including negatively charged bubble and positively charged bubble) also investigated through the change of algal morphology (i.e. size distribution and shape). Interestingly, in terms of three differing shapes, positively charged bubble functioned of rearranging the size distribution of filamentous algae by forming many smaller cells. Also, after positive bubble flotation, only filamentous algae changed its shapes to shorter filamentous algae and spherical-likely being. In addition, under stress environment, spherical and/ or spherical-likely shaped algae were considered as the most ideal existing configure. The discussion for dividing filamentous cells was deeply focused through possible mechanism when they attached with positively charged bubble. The collision of positive bubbles and filamentous cells occurs via two steps, they are 1) breakup of the chain-like cells and 2) attachment of the detached shorter algae to the bubbles, which then float to the surface.